INCREASING THE SHARE OF RENEWABLES THROUGH ADSORPTION SOLAR COOLING: A VALIDATED CASE STUDY

Valeria Palomba[a,b] , Salvatore Vasta[a], Angelo Freni[a] , Quanwen Pan[c], Ruzhu Wang[c], Xiaoqiang Zhai[c]

[a] CNR-ITAE Institute for Advanced Energy Technologies, Messina

[b] Department of Engineering, University of Messina

[c] Institute of Refrigeration and Cryogenics , Shanghai Jiao Tong University

ABSTRACT

Tools and experience on solar thermal cooling system sizing and design are still limited, as less than one thousand plants have been built until now. In this paper, a design tool for mid-size thermal solar cooling systems is presented. The tool consists of a model realised in TRNSYS and validated using the data of a real solar air conditioning system installed in the green building of Shanghai Research Institute of Building Science. Characteristic features of the system are the use of adsorption chillers driven by low-temperature solar heat from U-type and heat pipe evacuated solar collectors. The model has subsequently been employed for a technical analysis: the most relevant parameters have been varied and figures of merit calculated. An energy analysis has been performed for 6 reference cities, differing for climates and latitudes, highlighting the possibility to use only renewable energy for cooling purposes. Eventually, the systems have been compared with reference ones. Comparison highlighted that considerable savings in primary energy and CO_2 emissions can be achieved: 0.97 MWh per installed square meter of solar collectors and up to 22 tons of CO_2 annually, thus indicating a great potential for increasing energy efficiency and reduce CO_2 emissions.

Keywords: solar cooling; adsorption; energy analysis; TRNSYS

NOMENCLATURE

a	heat transfer area per unit volume, $m^2\ m^{-3}$
A	area, m^2
Ct	cooling tower constant, dimensionless
E	energy, kWh
G	total solar radiant power, W/m^2
h	hours, h
I	total incident irradiation, kWh/m^2
k	product of total heat transfer coefficient and heat transfer area, $kg\ s^{-1}\ m^{-2}$
L	liquid flow rate in the tower, $kg\ s^{-1}$
m	mass, kg
P	power, W
R	air flow rate in the tower, $kg\ s^{-1}$
T	temperature, °C
V	heat transfer volume in tower, m^3
x	exponent for cooling tower L/G ratio in context of experimental correlations, dimensionless

Subscripts

a	ambient
ADS	adsorber
chw	chilled water
cs	cooling season
el	electric
hp	heat pipe
hr	heat rejection
hs	heating season
in	inlet temperature
max	maximum
pd	production and distribution
sc	solar collectors
sens	sensible
sp	specific
U	U-type
y	annual

Greek symbols

α	leakage rate, dimensionless
γ	fraction of power, dimensionless
η	efficiency, dimensionless
θ	inclination, degree

Abbreviations

BF	bypass fraction, dimensionless
CO_2	carbon dioxide
COP	coefficient of performance, dimensionless
EER	energy efficiency ratio, dimensionless
GWP	global warming potential, kg_{CO2} kg^{-1}
PE	primary energy consumption, Wh
SCF	solar cooling fraction, dimensionless
SHF	solar heating fraction, dimensionless
SF	solar fraction, dimensionless
UF	utilization factor, m^2

1. INTRODUCTION

Reduction of CO_2 emissions and GHG emissions is, in today's world, a primary goal to be pursued, which is also the focus of the energy policies of many countries, as recently stated by COP21 agreement [1]. Tertiary and residential fields alone account for 40% of total global energy demand, with demand for space heating increasing by 2.6% per year and that for cooling by up to 6% per year [2]. The vast majority of such demand is covered by traditional vapour compression systems, employing R404 or R410a as refrigerant, which have a GWP of 3922 and 2090 respectively [3]. Ever-growing installed capacity has also lead to overload of national electric grids and black-outs, especially during summer [4].

In such a background, solar thermal systems can be considered a viable and environmentally friendly alternative, since they allow to exploit solar energy instead of electricity from fossil fuels, for air conditioning purposes. Moreover, in most of the cases, the availability of solar radiation and demand for cooling match [5]. Indeed, basic working principle of a solar cooling system is quite simple: it consists of a solar collector field used to provide hot fluid to a thermally driven unit, whose output is chilled water that can be used in a cold delivery system (e.g. fan coils or radiant floor and celing). Different alternatives and layouts have been proposed during the years, both for open systems solutions and closed systems [6]. The various technologies studied during the last decade include absorption systems [6, 7], adsorption systems [7, 8] and solid or liquid desiccant ones [9-11]. Moreover, hybrid solutions coupling the different technologies (e.g. desiccant-adsorption systems) have also been considered [6].

An extensive description of technologies available on the market, research trends and a classification of possible layout and solutions available in solar cooling and heating technologies is given in [7, 8]. Among the technologies for solar space heating and cooling available, single-stage and double-stage absorption chillers have the major share in the market [9-14]. They can be mainly distinguished in H_2O/LiBr and NH_3/H_2O systems, the former more common in residential applications since they need a lower driving temperature (< 100°C) [15]. However, they exhibit crystallization problems under some operating conditions. Double-effect ammonia chillers, among sorption technologies, have the highest COP (up to 1.2), but only when concentrating solar collectors for high temperature fluid production are available [5]. Adsorption units are generally characterised by a lower COP than the absorption ones but, instead, possess some additional benefits, since they can be driven by very low temperatures heat sources(< 70°C), do not have crystallization problems and employ water as refrigerant, which reduces corrosion problems and maintenance procedures [6]. Currently, they represent the most promising choice, and a lot of effort has then been put in R&D, with the goals of increasing efficiency of the systems and specific power, as to realize more compact units as described in [16-19]. Such research effort has led also to the development of products in small and medium sizes that are now available on the market [20, 21], together with comprehensive kits, meant for an easier installation. As a result, a growing trend has been observed, especially in newly-developing countries such as China, Turkey and Brazil [2]. A detailed description of market situation and future scenarios regarding solar cooling and heating technology can be found in [6].

Several studies are available in literature, aimed at proving the technical and economic feasibility of solar thermal cooling systems under various conditions. In [22], Eicker et al. developed a dynamic model for the systematic analysis of solar cooling systems under various climatic conditions covering most of global regions. Results demonstrated that, for southern Countries, solar cooling systems can be viable (DPT < 10 years) if incentives to reduce capital cost to 30-50% are applied. The same authors, in [23] compared solar thermal and solar PV systems for space cooling under typical office load conditions and found out that, if no feed-in tariff is applied for PV system, payback time of the two solutions are comparable. Hartmann et al. have proposed the same kind of analysis in [24], comparing solar thermal and solar PV solutions in 2 reference cities, Freiburg and Madrid. Results showed that primary energy savings up to 60% could be obtained by using the thermal system. Moreover, utilization of solar collectors also during winter proved to be a key factor. Mohan et al. [25] analysed a polygeneration system to simultaneously produce cooling, clean water and domestic hot water by coupling of membranes and an absorption chillers in climatic conditions of Saudi Arabia. Economic analysis performed demonstrated that payback time of 9 years can be achieved without financial support, and lower payback time (6.8 years) are possible if discounts on capital costs are considered. Vasta et al. [26, 27] analysed different layout solutions for a solar thermal cooling systems with an adsorption chillers at different Italian latitudes. Results of economic analysis showed that, when public incentives are applied, the system can be competitive with other solutions e.g. PV cooling. Reda et al. in [28] have performed an analysis for the Scandinavian climate, considering a solar thermal solution with absorption chiller and district heating, the main outcome being that the utilization of solar

cooling system can lead to a "power peak shaving" phenomena on the grid and partially solve the problems due to the excessive electricity consumption during summer. Moreover, Baniyounes et al. [29] assessed the feasibility of a solar assisted thermal system employing single effect absorption chiller, finding out that with 18 m^2 solar collector and a 1.8 m^3 thermal storage, 80% of primary energy savings, compared to a reference system, can be achieved. In [30], Al-Alili et al. have analysed a solar thermal system for Abu Dhabi climate, finding that to get about 50% energy savings in comparison to a traditional system, about 6 m^2 of solar thermal collectors should be installed for each kW of cold to be produced

Apart from TRNSYS analysis, validation studies on different systems have been reported as well. In [31], Praene et al. present the simulation and the results from field tests of a solar-driven 30 kW $LiBr/H_2O$ single-effect absorption cooling system. In [32], Muye et al. analysed, through TRNSYS simulation and field tests, a solar cooling system employing an absorption chiller and a scroll expander, employing biomass as back-up unit, in Spanish climate, with an overall seasonal efficiency in the range of 6-8% and a solar fraction around 20-30%. In [33], Buonomano et al. reported the dynamic simulation and experimental results of a solar cooling plant employing flat-plate solar thermal collectors and a double-effect absorption chiller installed in Saudi Arabia. More experimental investigations have been collected in the review by Aliane et al. [34]. However, all experimental investigations and validations have been performed only on systems employing absorption chillers. As far as authors know, no report on experimental validation of a solar-driven thermal system employing adsorption chillers has been reported in literature. This represents a significant gap, since the use of adsorption chillers is becoming relevant and the design of systems based on such technology requires reliable simulation tools.

In such a context, aim of this paper is then to present a modelling tool realised in TRNSYS, which can be applied for the design and the evaluation of solar thermal system employing adsorption units. With the goal of realising a reliable tool, useful for energy and technical analysis on solar cooling systems, it has been firstly designed on the basis of a real solar cooling system, installed in the green building of Shanghai Research Institute of Building Science. Such dynamic model has been validated by using the experimental data collected on the installation site. Since the model proved to be able to reproduce the behaviour of the real system, it has then generalised, in terms of installation site and load profile, and used for energy calculations and environmental analysis aimed at assessing the potential savings, such as primary energy, and benefits from renewable energy use. The distinguishing feature of the technical analysis performed is the sizing and comparison of the systems considering high solar fractions, while up to now most techno-economic analysis have been based on low solar fractions, focusing more on the optimization of the operating parameters. To this aim, different installation places and technical parameters have been considered, as to draw some analysis of general interest. Results showed that, for all the warmer climates, consistent savings and environmental benefits arise from solar cooling, making it one of the technologies to be considered in view of a global scheme for CO_2 reduction and renewable share increase.

2. SYSTEM DESCRIPTION

In 2007, an integrated solar energy system for heating, air conditioning, natural ventilation and hot water supply was built in the green building of Shanghai Research Institute of Building Science, which is situated in Xinzhuang, Shanghai, as a demonstration project. The flow diagram of the integrated solar energy system is shown in Figure 1. 150 m^2 solar collectors were set up on the roof of the green building for the use of 460 m^2 building area, wherein 90 m^2 U-type evacuated tubular solar collectors were placed on the west side (SCW) and the other 60 m^2 heat pipe evacuated tubular solar collectors were placed on the east side (SCE). For the efficient utilization of solar energy, those solar collectors were mounted to face due south and tilted at an angle of 40° to the ground surface. A 2.5 m^3 hot water tank (WT) was adopted to collect solar heat and provide hot water for the whole system. Two 8.5 kW silica gel-water adsorption chillers (AD),

which are capable of working from 55 °C to 95 °C, were used to provide the chilled water for air conditioning and they are cooled by a cooling tower (CT). Four pumps (P) were employed to maintain the water circuits, wherein P1 and P2 are the two solar collecting pumps, P3 and P4 are hot water pump and cooling water pump, respectively. Several valves were installed on the water pipes to realize the mode switch of the whole system. A detailed description of the system is reported in [35] and [36], while a picture of the installation is shown in Figure 2.

According to different seasons, the integrated solar energy system can be switched to different operating modes:

(1) In summer, adsorption chillers are powered by the solar hot water and produce the chilled water for air conditioning. The air conditioning system of the green building is a hybrid system which is composed of a liquid desiccant system and the solar adsorption air conditioning system. The latent cooling load is taken on by the liquid desiccant system, which is constructed by Shanghai Research Institute of Building Science. The sensible cooling load is met by the solar adsorption air conditioning system described above. Thereby, cooling and humidity loads are processed independently, and the fan coils inside air-conditioned rooms implement only the dry operating mode.

(2) In winter, solar hot water is delivered to the floor radiation heating system and used to satisfy heating load of the green building;

(3) In transitional seasons, solar hot water is pumped into finned tube heat exchangers in the stack of green building to induce stack pressure, which is capable of improving natural ventilation.

(4) The system can also supply hot water as long as a heat exchanger is installed in the hot water circuit.

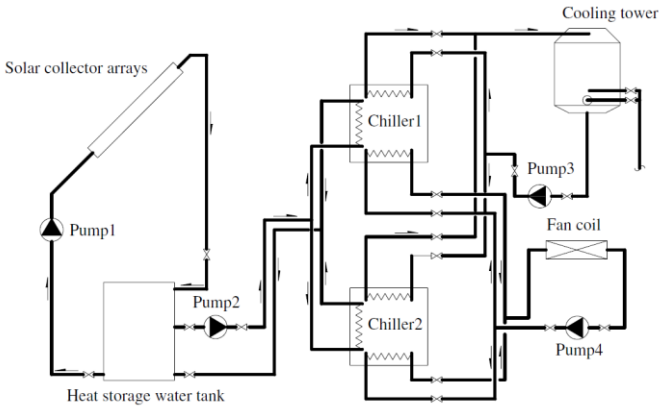

Figure 1. The flow diagram of the integrated solar energy system

Figure 2: The installed solar cooling system in Shanghai.

3. THE MODELLED SYSTEM

The analysed system was modelled by means of the commercial software TRNSYS, a specific tool designed to realise dynamic simulations of HVAC and complex energy systems [37]. The layout of the simulated system used for validation is that described in Figure 1. In Table I, a list of all the TRNSYS type employed for the simulation is shown, while details on some among the most important types are given in the appendix.

Table I: List of TRNSYS types used in the models

Element	TRNSYS Type	Element	TRNSYS Type
Solar collectors	1a	Variable speed pumps	110
Meteonorm weather data	15-2	Wet cooling tower	510
Psychrometric properties	33e	Fan coils	508h
Effective sky temperature	69b	Building	56
Adsorption chiller	909	Season schedule for heat/cool	515
Thermal storage tank	60	Hourly schedule	14h

A summary of the typical values in the loops of the system is given in Table II, in terms of temperatures and flow rates. The values reported in the table are the average values over the operating hours during summer season.

Table II: main parameters in the circuits of the modelled system.

Circuit	Temperature [°C]	Mass flow rate [kg/s]
1/ Solar collectors inlet	60	1.25 kg/s
2/ Solar collectors outlet	65	1.25 kg/s
3/Hot water chiller inlet	65	1.0 kg/s
4/Hot water chiller outlet	57	1.0 kg/s
5/Heat rejection chiller inlet	20-38	1.38 kg/s
6/Heat rejection chiller outlet	24-42	1.38 kg/s
7/Low temperature chiller inlet	12	0.42 kg/s
8/Low temperature chiller outlet	15	0.42 kg/s

For validation purposes, a first series of simulation was realised, for the summer season (May to October) considering two different cases:

- Solar field entirely made up of heat pipe collectors;
- Solar field entirely made up of U-type collectors.

Results, in terms of efficiency as a function of temperatures and solar radiation, are presented in Figure 3 and 4 respectively. The values from simulations are compared with the experimental data described in [36]. What emerges from the figures, is that a good correspondence between experimental and calculated data exists, for both types of solar collectors, thus allowing to conclude that the employed model is suitable for reproducing of the effective behaviour of the solar thermal side of the system.

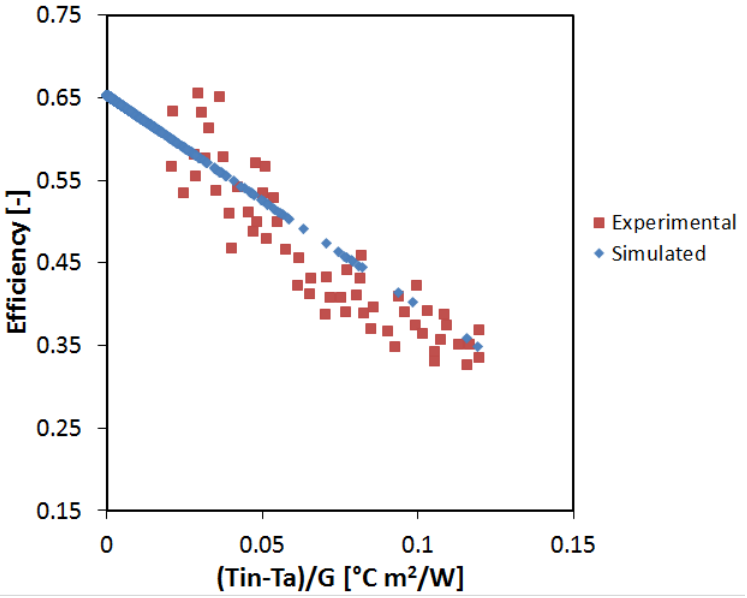

Figure 3: Simulated and experimental efficiency of heat pipe solar collectors as a function of temperature difference between inlet to collectors, ambient temperature and solar incident radiation on the surface.

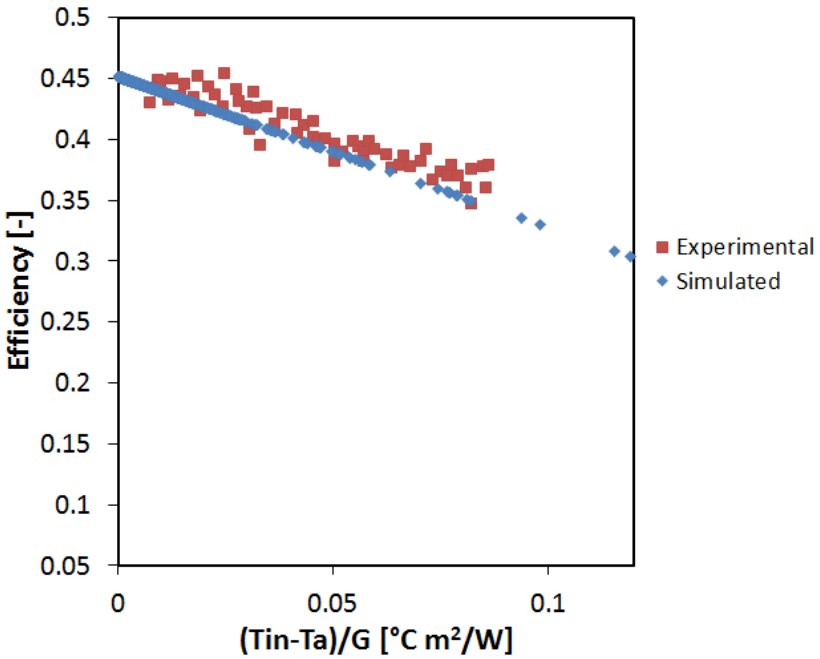

Figure 4: Simulated and experimental efficiency of U-type solar collectors as a function of temperature difference between inlet to collectors, ambient temperature and solar incident radiation on the surface.

Afterwards, simulations according to the actual layout of the system have been realised. In Figure 5 are reported the trends for inlet and outlet temperatures of the driving circuit of the adsorption chillers, which have been compared to the experimental data available in [35]. Results of the simulation are in good agreement with experimental ones, showing errors lower than 10%. As expected, in experimental data some sudden drops of temperature are observed, corresponding to the half cycles of the adsorption chillers and the consequent change between the beds adsorbing and desorbing. Such a trend is not detectable in simulated data, since Type 909, which has been used for the model of the adsorption chiller, only operates an energy balance of the system on the basis of the temperatures of the driving circuit, the cooling loop and chilled water inlet [37].

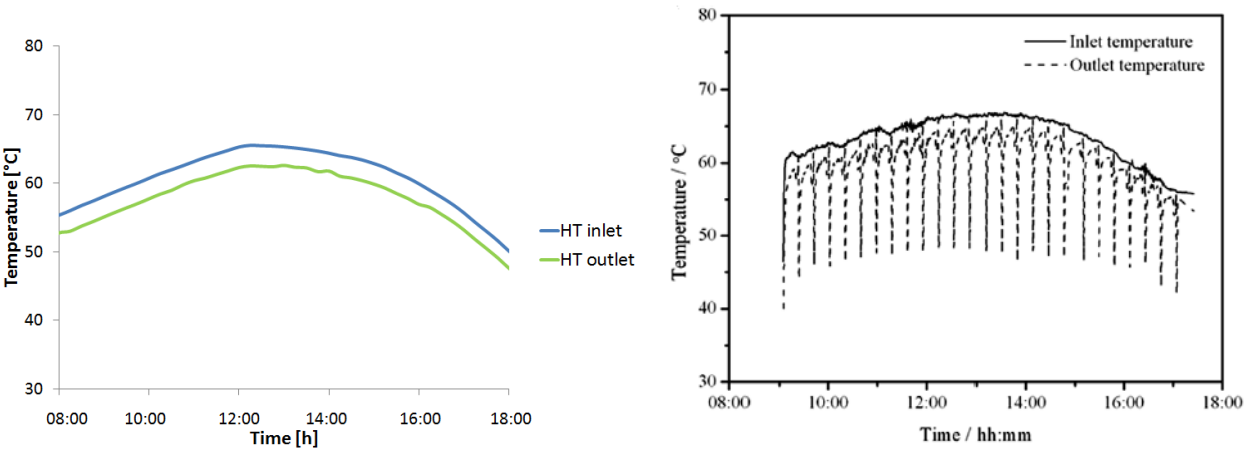

Figure 5: Comparison of inlet and outlet temperatures of the driving circuit of adsorption chillers, left: simulation, right: experimental data taken from [35]

In Figure 6 is reported also a comparison between the simulated cooling load for one reference day and the experimental ones. The simulated loads have been taken as the output of TRNSYS model for the sensible load of type 56, while the experimental ones correspond to the instantaneous power outlet from the chilled water circuit of the adsorption chillers.

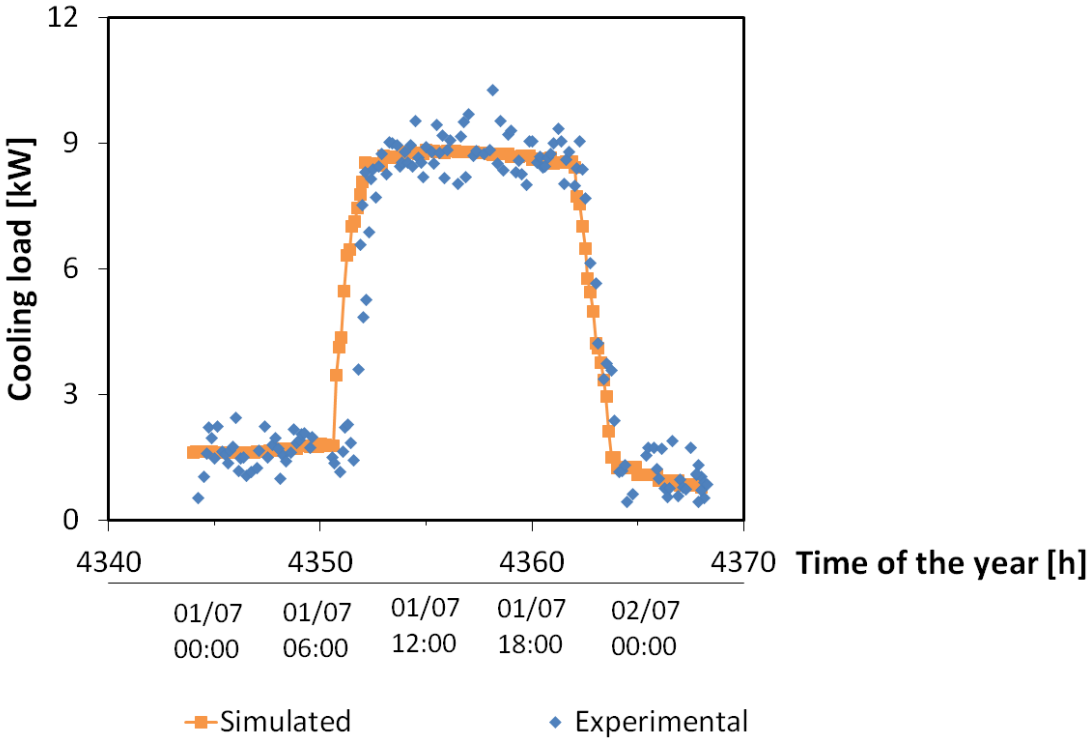

Figure 6: Comparison of cooling load of the building for one typical day in July from experimental data and simulations.

As shown in this section, the developed model could represent a viable tool for both the design and the analysis of solar cooling systems, reporting reliable data comparable with experimental ones. For the purpose of a more complete analysis of solar cooling systems in general, that will be presented in the next sections, it is worth noticing that load of the building has been introduced as a load profile instead that by detailed modelling of the building. This choice makes the tool easily adaptable to a wide range of conditions. Moreover, control logic implemented, which has been derived according to the real operation of the system installed in Shanghai, could be easily changed as well, thus determining a complete versatility of the tool.

4. RESULTS AND DISCUSSION

Aim of the technical, energetic and environmental analysis, which will be developed in the following sections, is to quantify the contribution of renewable energy to the whole HVAC system, highlight their possible level of exploitation for the chosen applications and assess the potential benefits of solar cooling technology towards a major share of renewable energy utilization. To this purpose, rather than a detailed technical analysis regarding all the components, energy utilization and solar radiation exploitation will be privileged. All the figures of performance employed for the evaluation of the system have been defined taking into account such criterion.

4.1 TECHNICAL ANALYSIS

The developed model could serve for a more general analysis of systems presenting the same features, in terms of load and occupation profiles. It is worth noticing that the layout considered represents the standard one, with solar collectors connected to a storage tank, from which an adsorption chiller takes hot water [4]. Moreover, it is easily verified that the defined load profile can be applied to a wide variety of buildings, such as a recently-built condominium in Italy or multi-family houses in Spain [38].

As previously stated, the main outcome meant for the analysis is to explore the possibility of having a high share of renewables for heating and cooling purposes, and indicate the conditions under which it is feasible. First, an energy analysis for the city of Shanghai is presented. The main parameters analysed are the efficiency of solar collectors and the solar fraction: regarding the former, the effect of the type of solar collectors and their area on the total energy exploitable have been assessed. Regarding the latter, the solar fractions under cooling and heating seasons have been calculated and, eventually, a general analysis on annual basis has been assessed.

Once a configuration able to give solar cooling fraction of about 1 in Shanghai has been identified, it has been applied to six cities at different latitudes, both in the northern and southern hemisphere, with the aim of comparing the results, in terms of renewables share in different climates. For all the cities, an environmental analysis has been also performed and the results presented.

4.1.1 Efficiency of solar collectors

In Figure 7, the efficiency of solar collectors is represented for 6 different solar field areas: 25 m^2, 50 m^2, 100 m^2, 150 m^2, 200 m^2, 240 m^2. An overall efficiency of the solar field, considering both types of solar collectors installed, has been calculated as:

$$\eta = \frac{E_{collectors}}{I_{\theta} A_{collectors}} \quad (1)$$

Where, the term $I_{\theta,\gamma}$ represents the instantaneous incident radiation on the surface, taken from the weather data for each location, while the energy of solar collectors has been calculated as a function of the inlet and outlet temperatures of the collectors and the mass flow rate to the arrays of collectors.

It should be remarked that the solar thermal field is organised in strings, each one containing 5 collectors. When increasing (or decreasing) the area of the solar thermal field with respect to the existing system in Shanghai, the collectors were added (or removed) in such a manner that they are connected as new strings in parallel with the existing ones. Such a choice, together with the control of the pump speed which has been previously discussed, allows to maintain the desired value of temperature in the tank, almost constant, in the various cases, thus keeping also the maximum driving temperatures of the chiller at a fixed level.

The volume of the storage tank has also been varied during simulations with different solar field areas: as shown in [26], for a fixed solar field area, the influence of storage volume is negligible both on solar fraction and electric COP of the whole system. For this reason, volume variation has been taken into account only to compensate for the higher energy to be stored: for each case, the volume of the storage corresponds to the minimum value to avoid stagnation [39], which is also beneficial in keeping the desired temperature level inside the tank. In [36], for the system under examination, the operation with or without heat storage has been analysed: when heat storage was present, a more constant inlet to the adsorption chiller is

accomplished, but no evident difference in the operation or performance operation of the system has been detected.

Values of storage volumes employed for the different simulations are reported in Table III.

The results of the simulations, summarised in Figure 7, show the average efficiency calculated for the operating hours of the solar cooling system. The detail on when the solar circuit is operated are given in appendix. It can be seen that the best performance is achieved when installing U-type evacuated tube solar collectors, which have a higher efficiency, reaching 0.61. As expected, annual efficiency of solar collectors is constant with respect to total area of the field, while the lowest performance is those of only HP collectors, with an average value of 0.43, and intermediate results obtained for the "mixed" solar field, as in the examined system.

Table III: Storage volumes for the different solar field areas simulated.

Solar field area [m^2]	Storage volume [m^3]
25	1
50	1.5
100	2
150	2.5
200	3
240	3.5

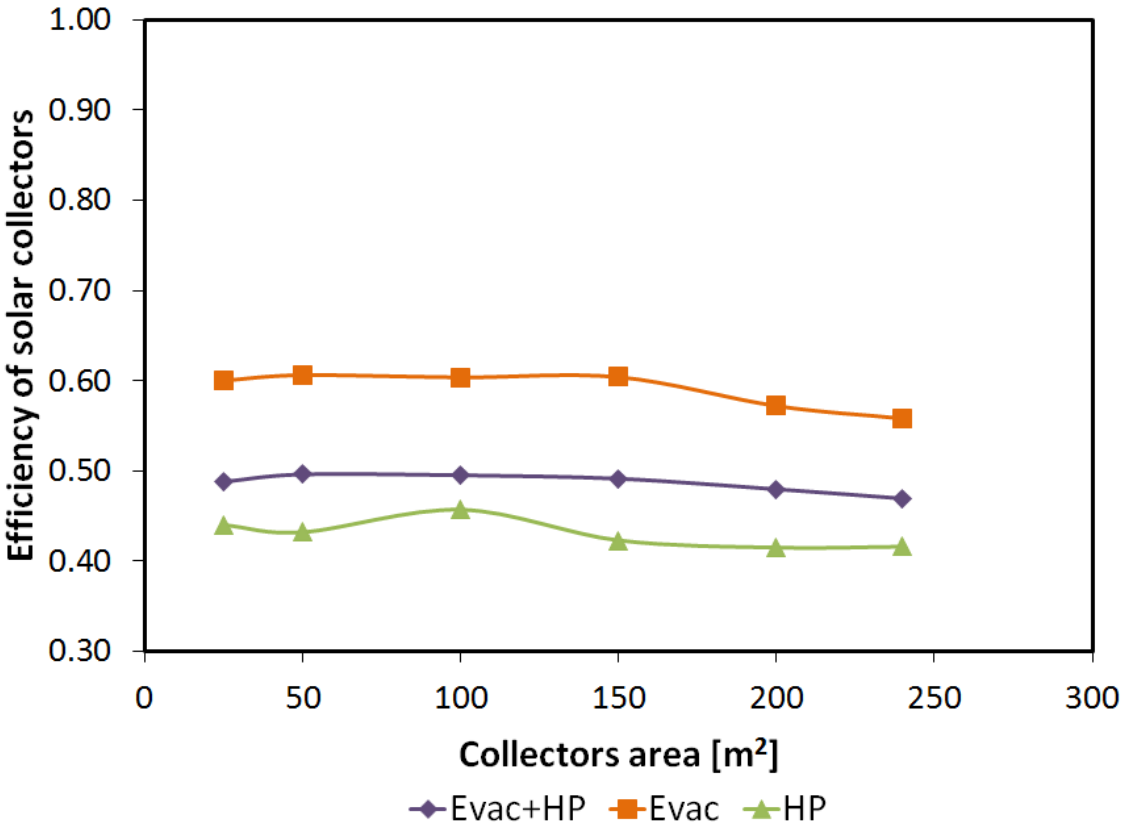

Figure 7: Efficiency of solar collectors as a function of solar field area for constant average temperature of the fluid inside the collectors.

4.1.2 Solar cooling fraction

The second parameter to be investigated is solar fraction, defined as the ratio between energy supplied by solar collectors during cooling season and the annual demand for driving the adsorption chiller for cooling production:

$$SCF = \frac{E_{collectors,cs}}{E_{\text{driving, ADS}, y}} \tag{2}$$

In particular, during simulation and data analysis, the season for cooling has been calculated as the one where the average daily cooling cooling load exceeded 3 kW for at least 7 consecutive days (1 week). The same criterion was used for the calculation of the heating season. The energy terms in the equation are obtained by integration of the output value suggested by TRNSYS over the time step. Results obtained are reported in Figure 8, where solar cooling fraction is reported, for all the three examined cases, as a function of solar collectors' area. As for the previous analysis, among the cases reported in terms of solar field area, 3 cases (25 m^2, 50 m^2, 100 m^2) have a solar extension lower than the actual system, which does not comprise any back-up chiller or heater, and 2 cases (200 m^2, 240 m^2) have a solar extension higher. In particular, for the system with 100 m^2 collectors area for all the examined scenarios, solar fraction is about 1, thus indicating a good match between demand coverage and solar energy availability. For the scenarios with higher extensions of solar field, excess heat exists, especially when the area of collectors exceeds 200 m^2. Indeed it is not technically nor economically beneficial to oversize the system in order to obtain solar fractions exceeding 1; on the contrary, it leads to extra costs due to the need of bigger components (pipes, pumps, storage tank). Aim of the presented analysis was to define under which design conditions, a system completely driven by renewable energy could be realised and, accordingly, the following analysis will be done considering a system having unitary solar fraction.

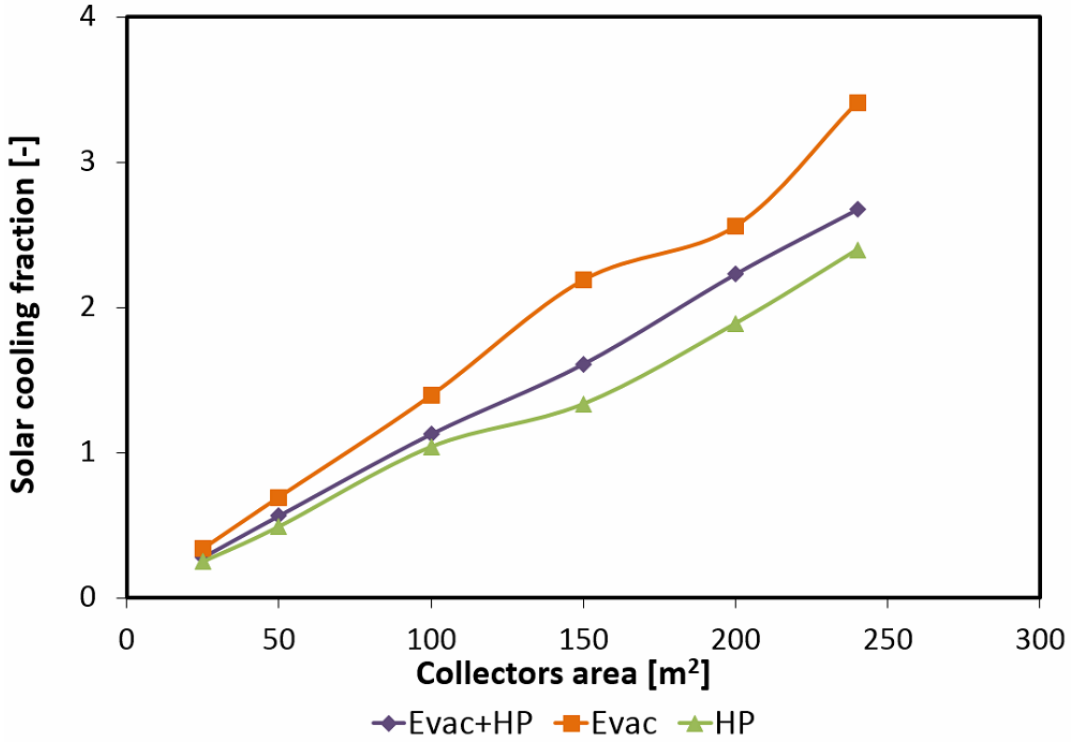

Figure 8: Solar cooling fraction as a function of solar field area.

4.1.3 Solar heating fraction

In analogy with what reported in the previous section, coverage by solar energy of winter demand for space heating has been assessed. In particular, as previously described, in such conditions, heat from solar panels is used for "free heating" of the building. It is worth noticing that, by using variable speed pumps like those included in the models, it is possible to assure that outlet from solar thermal collectors is maintained to the desired level.

Solar heating fraction has been defined as the ratio between the energy supplied during heating season by the solar collectors and the energy needed for space heating:

$$SHF = \frac{E_{collectors,\mathrm{hs}}}{E_{heating}} \tag{3}$$

As for summer season, winter season has been defined by the presence of a heating demand of at least 3 kW for one week. Results are reported in Figure 9, where it is possible to see that, for the analysed climate conditions, with the exception of the system with solar field area of 25 m^2, solar collectors are able to provide more energy than needed during winter.

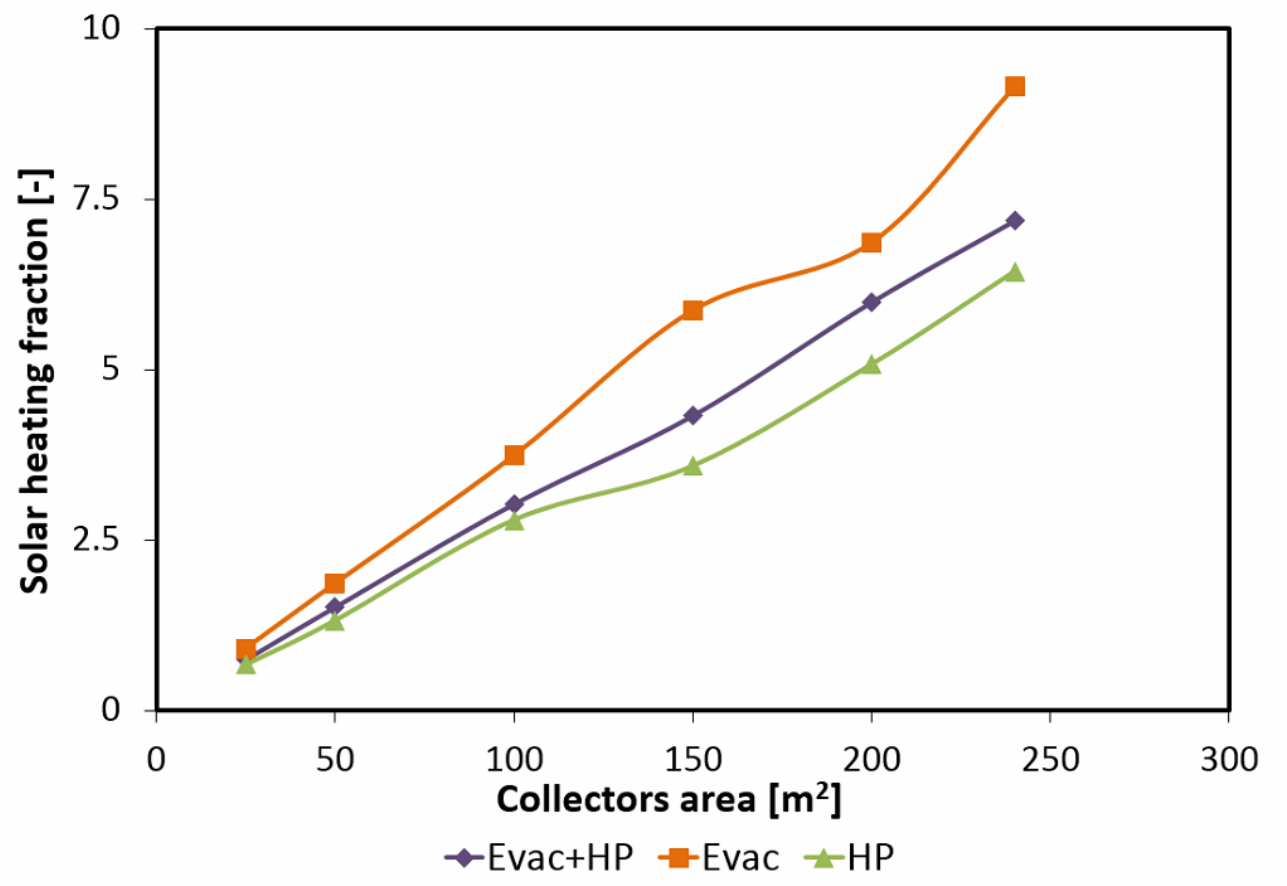

Figure 9: Solar heating fraction as a function of solar field area.

4.1.4 Solar fraction

The results presented for cooling and heating season were grouped considering total solar fraction, defined as the ratio between total energy supplied by solar collectors and those yearly needed for space heating and cooling:

$$SF = \frac{E_{collectors,y}}{E_{heating} + E_{driving,ADS,y}} \quad (4)$$

Results are summarised in Figure 10, presenting the same trend as the others, with the best combination being 100 m^2 for solar field extension. The results obtained are particularly interesting since they allow to understand that it is possible to design a system entirely powered by solar energy, in summer conditions and, where climatic conditions during winter are not extremely severe, as in most Mediterranean and tropical countries, even during throughout all the year.

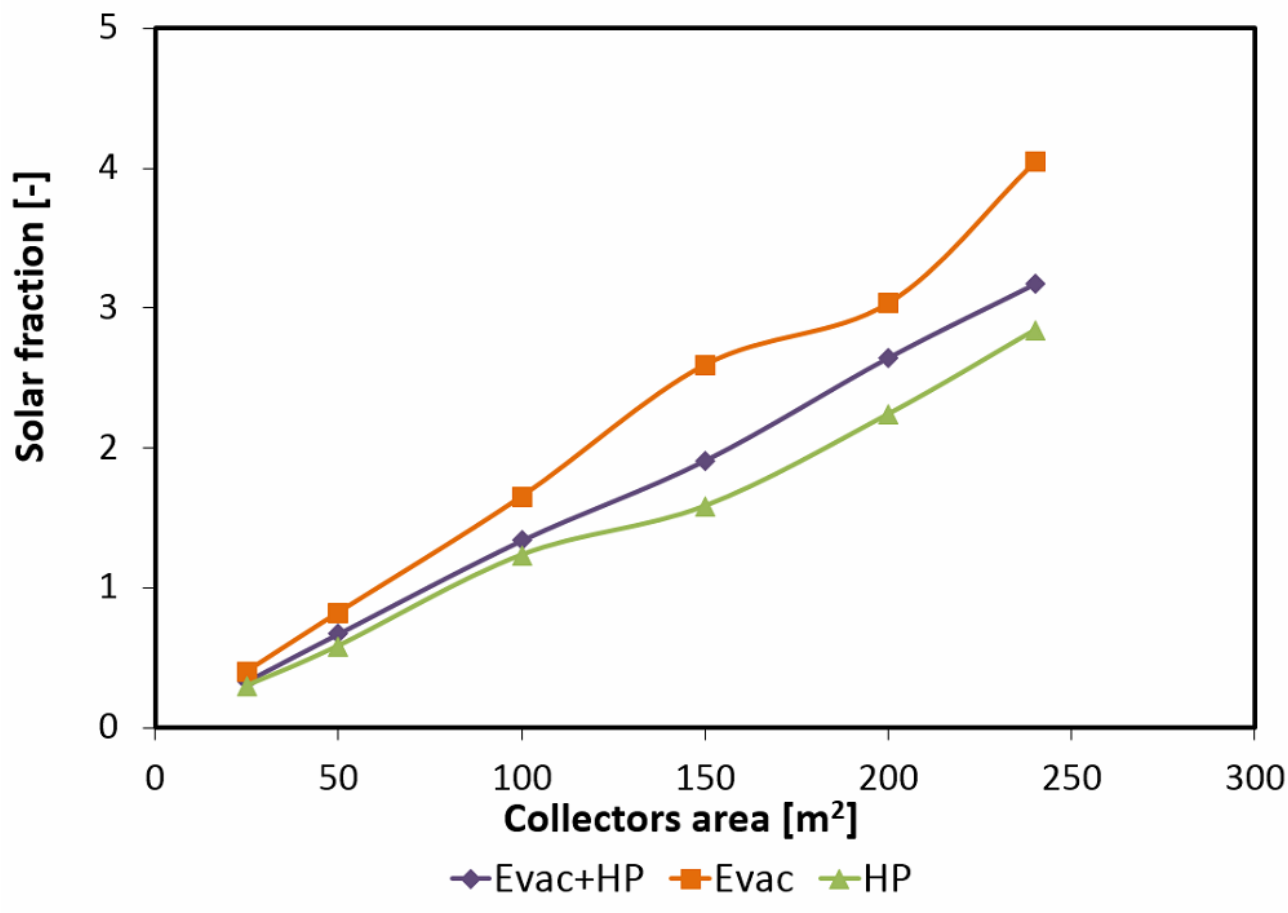

Figure 10: Total solar fraction as a function of solar field area.

4.1.5 Geographical installation

To conclude the technical analysis and draw some more general results, which will allow for a detailed energy analysis, 5 different locations have been considered, apart from Shanghai: Messina (Italy), Cape Town (South Africa), Caracas (Venezuela), Kuala Lumpur (Malaysia) and Munich (Germany). The selected cities are at different latitudes and present different climates: from tropical climate for the cities near the Equator, to continental one for Munich where heating load represents the most part of the demand of the year, to Cape Town where a substantial balance between heating and cooling demand exists. For each of the city, a standard configuration has been analysed, i.e. the one with U-type evacuated solar collectors for a total area of 100 m^2, which, for the city of Shanghai had evidenced the solar fraction closest to 1. To take into account the different latitudes of the cities, tilt angles of solar collectors has been varied according to what reported in [40]. Results are summarised in Table VI, in terms of solar cooling fraction and solar total

fraction. As expected, a wide variability of the investigated parameters can be obtained, considering the extremely different conditions of the various cities, but values of solar fraction, especially for cooling are still high, thus indicating the technical feasibility of a full solar fed system and its promising potential. In Table VI, seasonal COP of the adsorption chiller for each city has been introduced as well, for cooling mode. The COP is strongly influenced by external temperature, which, in turns, affects heat rejection temperature. The lowest value calculated is 0.28 in Kuala Lumpur, where the humid and hot climate negatively affects the performance of the chiller, while the highest value is the one found for Munich, where the external temperature never rises over 30°C, even during summer. Such values are certainly lower than those reported for absorption chillers [7], but the possibility of reaching high solar fractions, even with such a performance, further indicates the interest that adsorption technology might have in the future.

Table IV: Results of simulation for different cities

City	Latitude	Optimal tilt angle	Average yearly temperature [°C]	Seasonal Cooling COP	SCF	SF
Shanghai	31° N	40°	15.8	0.37	1.40	1.60
Caracas	10°N	10°	25.55	0.30	0.67	1.09
Cape Town	33° S	30°	18.47	0.34	1.80	2.61
Messina	38°N	30°	18.09	0.32	4.61	2.60
Munich	48° N	45°	16.16	0.38	4.65	5.46
Kuala Lumpur	2° N	10°	26.56	0.28	0.63	1.02

In order to obtain a parameter useful for the actual comparison and the design of the systems, a new different parameter has been introduced, the solar utilization factor, defined as the useful area of solar thermal collectors needed for the realisation of a solar cooling system with unitary solar fraction, for the examined conditions. It is worth noticing that, since for most of the examined cities summer cooling demand exceeds winter heating one, the obtained value would imply the satisfaction of heating demand as well. It has been calculated as:

$$UF = \frac{E_{driving,ADS,y}}{\frac{E_{collectors,cs}}{A_{collectors}}} \tag{5}$$

Which can be expressed also in terms of the solar area needed for each kW of cold produced:

$$UF_{sp} = \frac{E_{driving,ADS,y}}{\frac{E_{collectors,cs}}{A_{collectors}}} \cdot \frac{1}{\frac{E_{cold,ADS,y}}{h_{cs}}} \tag{6}$$

Considering that:

$$\frac{E_{collectors,cs}}{A_{collectors}} = I_{\theta,cs}\eta_{collectors,cs} \tag{7}$$

441 and
442
443 $$\frac{E_{driving,ADS,y}}{E_{cold,ADS,y}} = \frac{1}{COP_{ADS,av}} \quad (8)$$
444
445 It can be rewritten in terms of typical design parameters of the system as:
446
447 $$UF_{sp} = \frac{h_{cs}}{I_{\theta,cs}\eta_{collectors,cs}COP_{ADS,cs}} \quad (9)$$
448
449 Results are reported as a function of average temperature throughout the year for the examined cities in
450 Figure 11. Values obtained highlight that, for the areas with higher cooling demand, up to 8 m^2 are
451 necessary to produce 1 kW of cooling using only renewable energy, while values of 4 m^2 have been found
452 for Messina, which is in good agreement with what reported in [41], and Cape Town. In Munich,
453 apparently, the lowest area is needed to realise a solar cooling system. However, for the continental
454 climate, heating demand becomes the key parameter when designing a system and, therefore, it should be
455 considered of greater importance than for the other cities. Indeed, in Munich, for the examined
456 configuration (100 m^2 evacuated collectors, free heating during winter from solar collector), a solar heating
457 fraction of 0.38 has been found, indicating that the need for a space heating back up system is necessary in
458 this case. Fitting of simulated data has also been reported in Figure 11: it is possible to detect an increasing
459 trend for higher temperatures. In Figure 12, the cities are compared on the basis of annual incident
460 radiation on the surface of solar collectors: with the exception of Munich, the higher the annual incident
461 radiation, the lower the surface needed for the production of 1 kW_f. The results of Figure 12 and 13
462 indicate that both temperature and irradiation held a significant influence on the performance achievable
463 and sizing characteristic of a solar cooling system and should then be regarded, especially during the design
464 process.
465

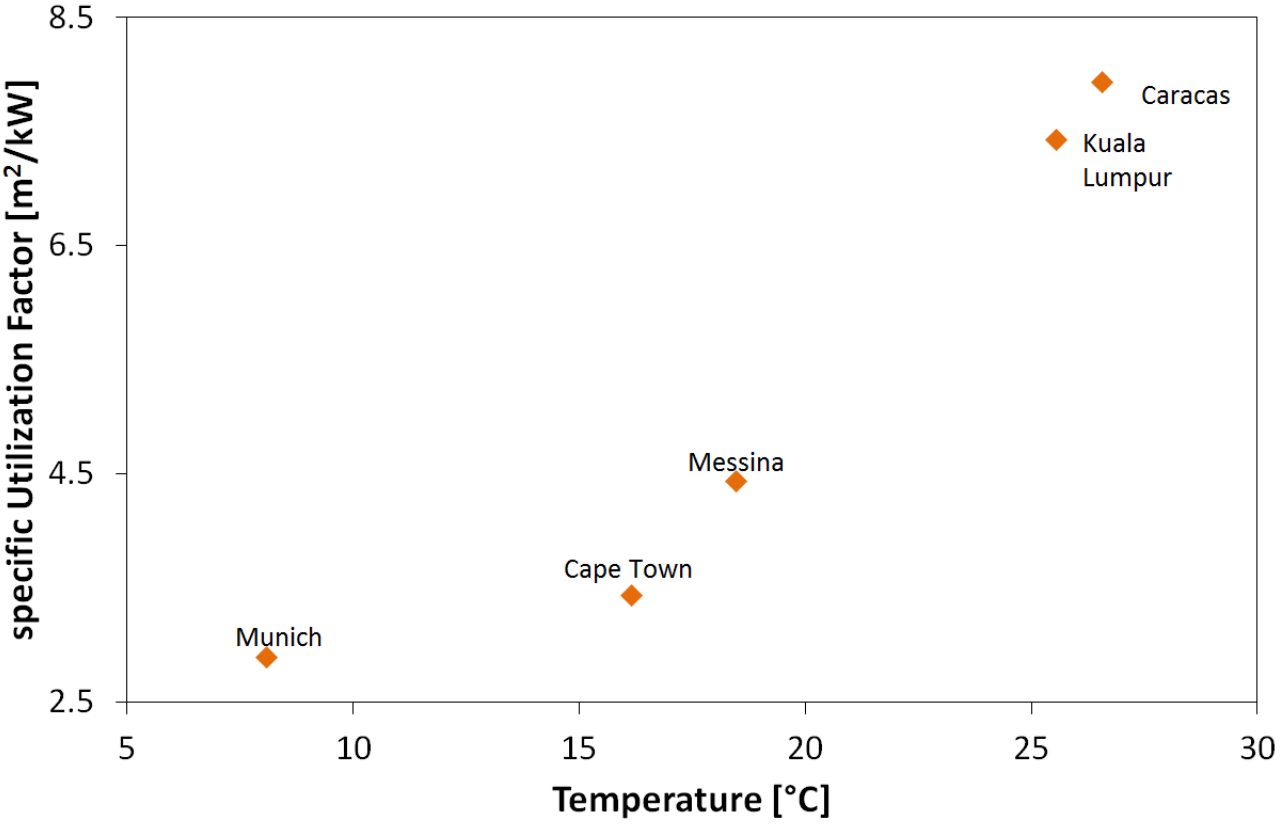

Figure 11: Specific utilization factor as a function of annual average temperature in the different cities.

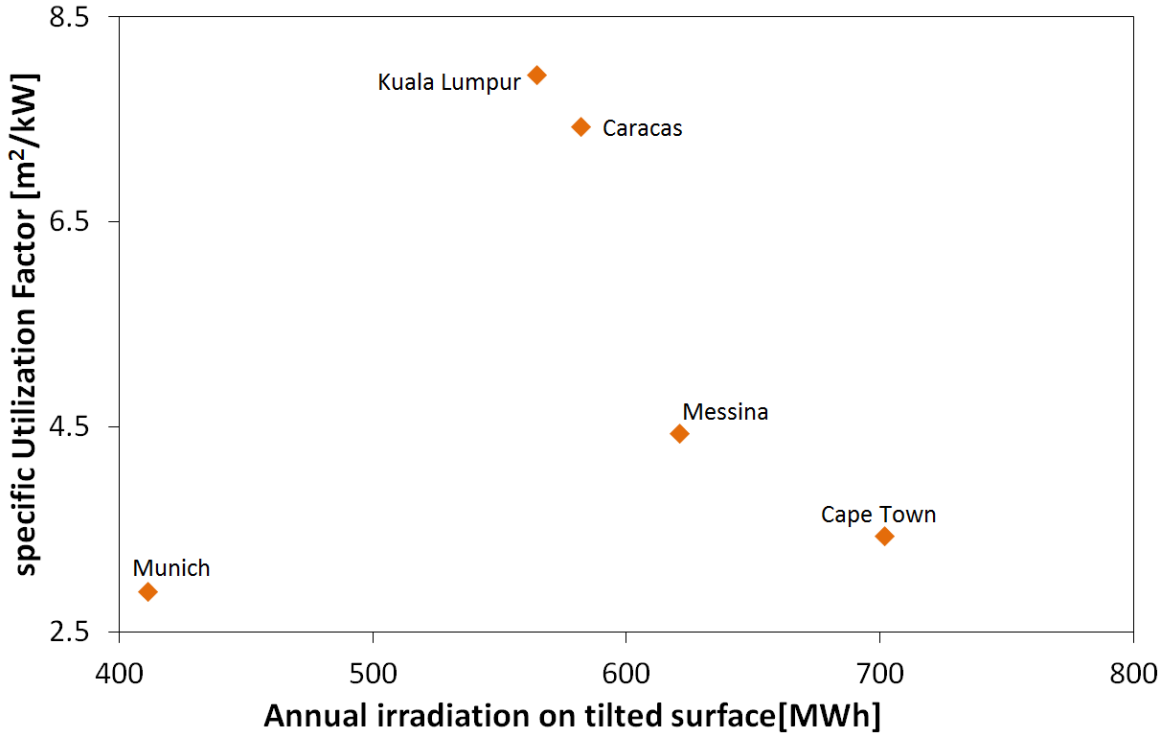

Figure 12: Specific utilization factor as a function of annual irradiation on the surface of solar collectors for the different cities.

5 ENERGY AND CO_2 EMISSIONS ANALYSIS

Purpose of the energy analysis is to compare, in terms of primary energy savings, the solar cooling system, examined for the various cities described in the previous section, with a traditional system employing an electric heat pump. Since the aim is to highlight the role of renewables for cooling and space heating, in simulating solar thermal systems it has been considered the area needed to obtain an annual solar fraction of about 1. The reference system is represented by a vapour compression R410 water cooled system. Like the solar thermal system, the electric-driven system has been simulated in TRNSYS employing the same weather data as the solar thermal system for the selected cities.

For a traditional system, the primary energy consumption is given by [14]:

$$PE_{traditional} = \left(\frac{\mathrm{E}_{cold\_demand}}{EER_{traditional}} + E_{wet\_tower} + E_{auxiliaries} \right) \frac{1}{\eta_{pd}} \tag{10}$$

Where:

$$E_{auxiliaries} = \frac{E_{pump,hr}}{\eta_{pumps}} \tag{11}$$

Instead, for solar thermal system:

$$PE_{solar\_thermal} = \left(E_{ADS,el} + E_{wet\_tower} + E_{auxiliaries} \right) \frac{1}{\eta_{pd}} \tag{12}$$

Where:

$$E_{auxiliaries} = \frac{E_{pump,\mathrm{solar}} + E_{pump,\mathrm{hr}} + E_{pump,\mathrm{chw}}}{\eta_{pumps}} \tag{13}$$

National efficiencies for production in public electricity have been taken from [42] and are reported in Table V.

Table VI: national energy efficiencies used in Equation 10.

City	National energy efficiency
Shanghai	0.32
Caracas	0.30
Messina	0.44
Munich	0.40
Cape Town	0.37
Kuala Lumpur	0.35

Primary energy savings calculated, and primary energy savings normalized for solar field area are reported in Table VI. It is worth noticing that, especially in the hottest regions, consistent savings, up to 1 MWh/y can be obtained for a single square meter of solar panel installed, thus indicating a great potential for increasing energy efficiency. Such particularly favourable results, especially for Caracas and Kuala Lumpur, are determined by three concurring factors: the high annual solar radiation, which allows for a consistent energy output from solar collectors, the existence of a constant cooling demand, for more than 280 days

per year, and a national efficiency of primary energy production which is significantly lower than those in countries like Germany and Italy.

Together with energy aspect, CO_2 emissions should be regarded when analysing a renewable energy-based system. The environmental performance was evaluated through an approach based on the equivalent carbon dioxide emissions (CO_2). The comparison is based on the avoided CO_2 emissions of the adsorption cooling system if compared to a traditional ones.

To this aim, avoided CO_2 emissions have been calculated taking into account both the direct emissions, due to the primary energy consumption over year, and the indirect emissions due to leakage of refrigerants, as:

$$\Delta CO_2 = CO_{2,\mathrm{trad}} - CO_{2,ads} = \frac{PE_{trad} - PE_{ADS}}{\eta_{CO_2}} + m_{R410a} \cdot GWP_{R410a} \cdot \alpha \qquad (14)$$

Data for calculations of CO_2 emissions from primary energy production are those taken from [43], while the following data have been defined used for calculations of indirect CO_2 emissions: refrigerant charge of 3.3 kg_{R410a} [44], GWP of 1924 [44] and leakage rate of 10%, which is typical of domestic air conditioning systems[45]. Results are reported in Table VI, where consistent amount of avoided emissions can be observed.

Table VI: Primary energy savings for the examined cities and avoided CO_2 emissions

City	Primary energy Savings [MWh/y]	Specific Primary Energy Savings [MWh/(m²y)]	tCO_2/y avoided
Shanghai	38	0.44	10.09
Caracas	115	0.97	22.35
Cape Town	28	0.63	5.09
Messina	6	0.37	1.71
Munich	13	0.76	3.87
Kuala Lumpur	95	0.75	22.81

CONCLUSIONS

In this paper, a useful and reliable design tool for thermally driven solar cooling systems has been presented. It is based on a TRNSYS model and has been successfully validated by using the data of a real solar system installed in Shanghai: the error found comparing simulated and real data lies in the range of 5-10 %.

The validated tool has been used to carry out a detailed energy analysis considering 5 different locations apart from Shanghai: Messina (Italy), Cape Town (South Africa), Caracas (Venezuela), Kuala Lumpur (Malaysia) and Munich (Germany).

For each of the city, a standard configuration has been analysed, varying at the same time some design parameters, such as tilt angles of solar collectors, thermal storage volume and the numbers of solar collectors.

Results have been analysed in terms of renewable energy exploitation, introducing the utilization factor, a parameter indicating the net area needed for production of 1 kW of cooling using only renewable energy. In high cooling demand areas, up to 8 m^2/kW are necessary (Kuala Lumpur, Caracas), while values of 4 m^2/kW have been found for mild climate areas (i.e. Messina). On the other hand, in continental climates (Munich), the heating demand becomes the key parameter and for Munich, considering the same area needed for cooling production with solar fraction 1, a solar heating fraction of 0.38 has been found, indicating the need of a space heating back up unit.

Finally, the systems have been compared with reference ones employing traditional vapour compression electric chillers. Comparison highlights that, especially in the warmer regions, considerable savings in terms of primary energy and CO_2 emission can be achieved. The energy and environmental analysis, show that is possible to yearly reduce the primary energy demand of almost 1 MWh per installed square meter of solar collectors and avoid the emission of more than 22 tons of CO_2 in the atmosphere. These values clearly indicate a great potential for increasing energy efficiency and reduce the carbon footprint of heating and cooling system by applying the solar technology.

APPENDIX: MODEL DESCRIPTION

In the present appendix, more detailed information on the model, TRNSYS types and the parameters used in the simulations are given. In Figure A.1, the flow sheet of the TRNSYS model including the main connections and types used is shown. In the following sections, the parameters and equations implemented are described; for the equations that are not indicated, the detailed procedures can be found in [36]. The time step chosen is 15 minutes.

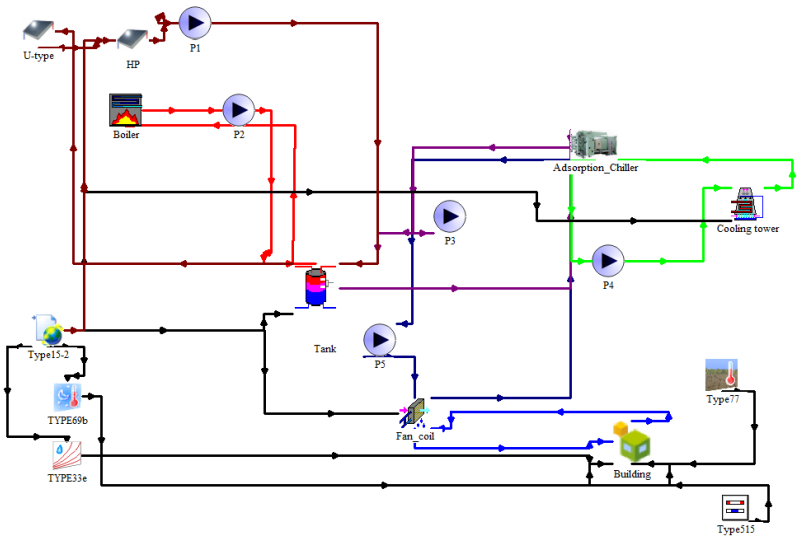

Figure A.1: schematic layout of the TRNSYS model employed.

Building

The building envelope has been simulated by means of TRNSYS type 56. In particular, two floors have been considered in calculation of the thermal needs: the ground floor with total surface of 335 m^2 and a total surface of 125 m^2 for the first floor, which corresponds to the offices served by the adsorption chillers. The main parameters implemented in TRNSYS are reported in Table A.1. Subsequently, the sensible loads of the buildings have been calculated for the entire year, and are depicted in Figure A.2, in the form of a load duration curve, by distinguishing heating and cooling contributions. The peak load found through

580 simulations is 17 kW, while the average one is about 8 kW, which is consistent with the sizing of the
581 adsorption chillers.

582 **Table A.1: parameters used in the simulation of the building**

583

Parameter	Unit	Value
Wall transmittance	$W/m^2 K$	0.35
Window transmittance	$W/m^2 K$	1.65
Roof transmittance	$W/m^2 K$	0.45
Floor transmittance	$W/m^2 K$	0.28
North wall area	m^2	106.87
South wall area	m^2	31.26
West wall area	m^2	31.26
East wall area	m^2	79.62
North window area	m^2	50.63
South window area	m^2	62.54
West window area	m^2	6.12
East window area	m^2	6.12
1^{st} floor area	m^2	335
2nd floor area	m^2	125
Total volume	m^3	728
Air changes	h^{-1}	0.30
Maximum ventilation rate	kg/h	1200
Heating season set-point	°C	20
Cooling season set-point	°C	26

584

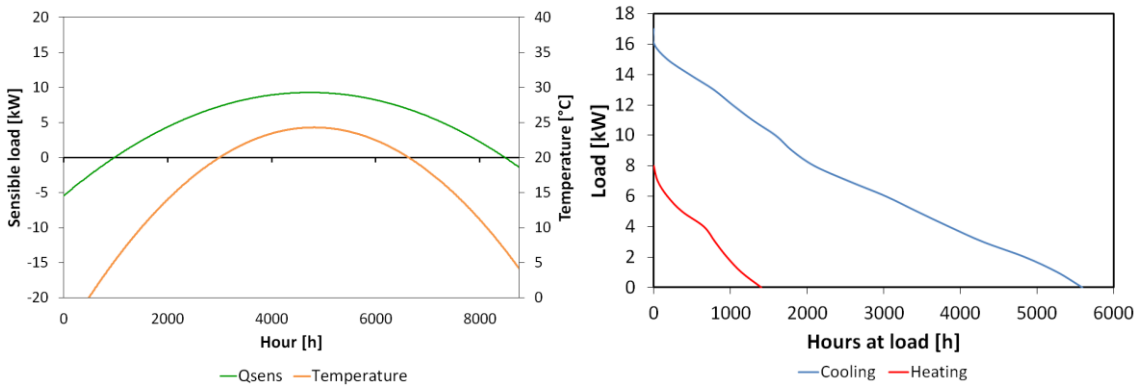

585

586 **Figure A.2: load demand and load duration curve for the building in Shanghai for the entire year.**

587 **Solar collectors**

588 The solar thermal field is realised by coupling two different types of solar collectors: U-type evacuated
589 collectors and heat pipe tubular collectors. Both have been modelled by definition of an equation for the
590 useful energy gain of the collector, based on experimental data, as described in [35].

591 For heat pipe collectors, efficiency was obtained as:

592
$$\eta_{HP} = 0.65 - \frac{2.94\left[\frac{W}{m^2 °C}\right](T_{sc} - T_a)[°C]}{I\left[\frac{W}{m^2}\right]} \qquad \text{(A.1)}$$

593 For U-type collectors:

594
$$\eta_{U} = 0.45 - \frac{1.10\left[\frac{W}{m^2 °C}\right](T_{sc} - T_a)[°C]}{I\left[\frac{W}{m^2}\right]} \qquad \text{(A.2)}$$

595 In both cases, for implementation in TRNSYS, a tested flow rate of 0.014 kg/(s m^2) has been used.

596 Such efficiency are corrected by TRNSYS routine, as described in [37] and more in details in [46], to take
597 into account the effect of effective flow rate, tilt angle of the collectors and the number of collectors in
598 series. For such a reason, the maximum efficiency of the arrays of collectors can, under certain conditions
599 (e.g. very high flow rate) exceed the maximum theoretical values of 0.65 and 0.45.

600 **Storage tank**

601 The modelled storage tank is a stratified storage with heat loss coefficient of 0.95 W/°C. Internal heat
602 exchangers have been considered for the connection of solar thermal circuit. For calculation on the thermal
603 storage system, TRNSYS routines divide the tank into nodes, an energy balance being performed on each of
604 them, as described in [36]. Dimensional parameters of the storage are given in Table A.2:

605

606

607

608

Table A.2: Parameters for the storage tanks used in the models

Parameter	Value
Heat exchanger surface area [m^2]	130
Storage volume [m^3]	2.5
Storage height [m]	2.2
Storage fluid	Water
Height of HEX inlet/outlet	0.10 m / 1.10 m
Height of inlet/outlet for adsorber circuit	0.10 m/ 0.75 m
Heat exchanger material	Copper
Heat exchanger length [m]	31.55
Heat exchanger diameter	¾”

Adsorption chiller

The environmental friendly silica gel-water adsorption chillers, used in the solar cooling system employs heat and mass recovery processes to improve the system performance. Each chiller is composed of three vacuum working chambers: two desorption/adsorption working chambers and one heat pipe working chamber. Only one vacuum valve is installed to fulfil the mass recovery between two desorption/adsorption working chambers. The evaporators are gravity heat pipe heat exchangers, which avoid using switch valves in chilled water circuit. A schematic layout of the system taken from [47] is shown in Figure A.3.

The chiller is capable of working under the heat source temperature from 55 °C to 95 °C. The nominal refrigeration capacity is 8.5 kW when the hot water temperature is 85 °C. A more detailed description of the chiller and its performance can be found in [48,49]. As an example, in Figure A.4, the plots reporting cooling capacity and COP as a function of heat rejection temperature, are shown. They are calculated with chilled water temperature of 15°C. It is worth noticing that, when heat rejection temperature is lower than 30 °C, cooling capacity exceeds the nominal one, and that the COP of the system keeps around 0.3 - 0.4 under most practical conditions.

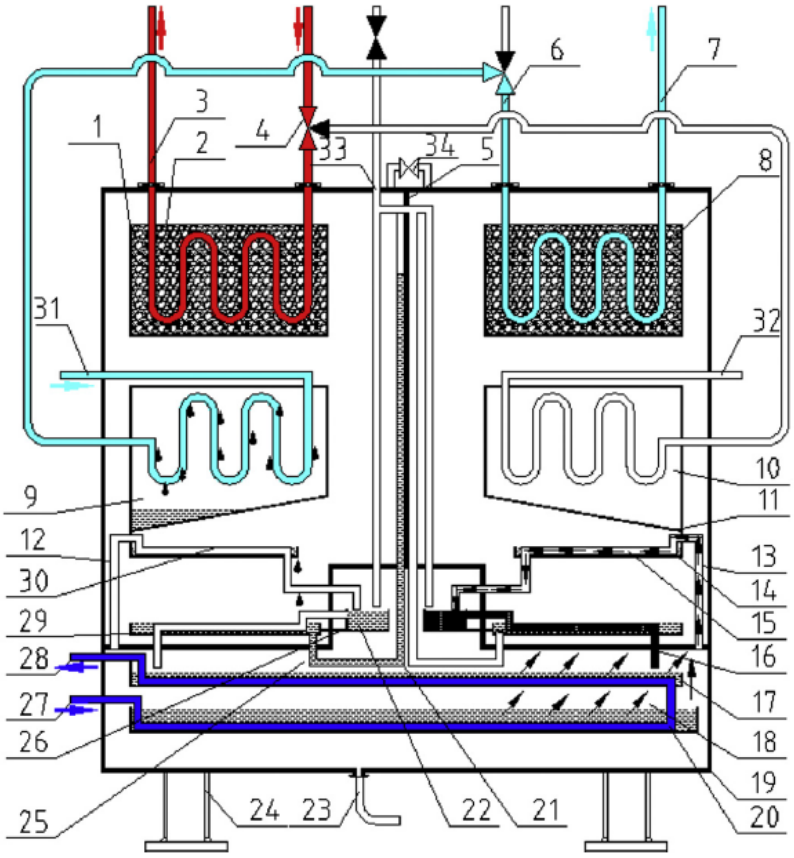

Figure A.3: The schematic diagram of adsorption chiller. The main components are: 1-left adsorber, 8-right adsorber, 9-left condenser, 10-right condenser, 18-evaporator, 34-mass recovery valve. [

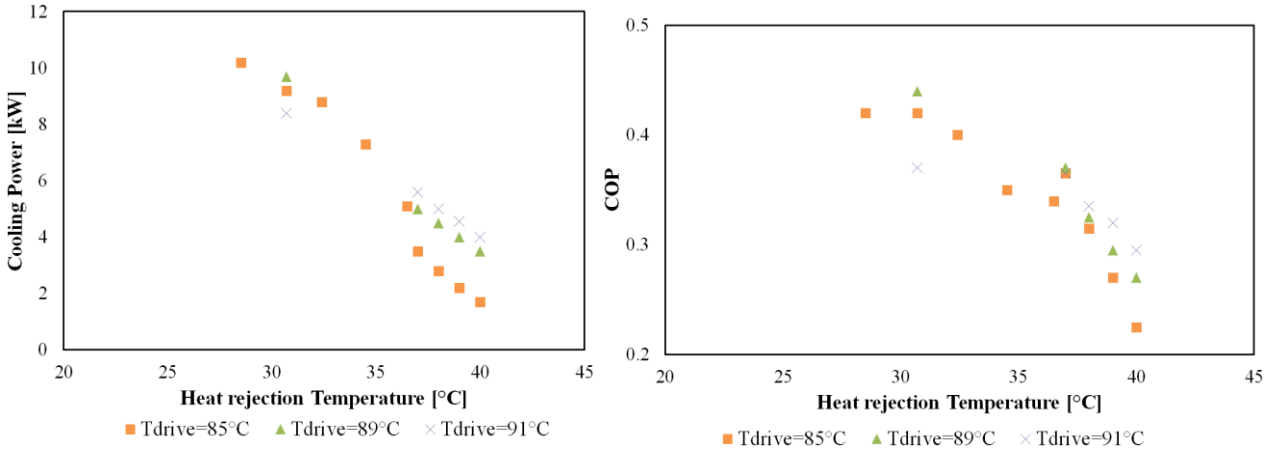

Figure A.4: Performance curves of the simulated adsorption chiller. On the left: cooling capacity as a function of heat rejection temperature. On the right: COP as a function of heat rejection temperature (chilled water outlet = 15°C).

The adsorption chiller has been simulated in TRNSYS with type 909, which employs a performance map: cooling capacity and COP under different conditions (in terms of driving temperature, chilled water temperature and heat rejection temperature) from experimental data measured have been implemented, the solver interpolating them to find the correspondent values for each instantaneous condition. In the present study, the ranges of temperatures considered for the construction of the performance map are: 60 °C-91 °C as driving temperature, 25 °C-40 °C as heat rejection and 12 °C-20 °C for chilled water.

Wet cooling tower

The cooling tower employed in the model is a mechanical-draft, single cell counterflow cooling tower with thermal capacity of 35 kW, with maximum electric power consumption of 1.8 kW. The heat and mass transfer performance of the cooling towers is given in terms of the NTU level achieved as function of the water to air flow rate ratio as follows [50]:

$$\frac{kaV}{L} = C_T \left(\frac{L}{R} \right)^{-x} \tag{A.3}$$

Since data from constructor did not include values for the mass transfer coefficient and exponent, data of 1.3 and 0.6 were employed, as suggested in [51].

Power consumed from the auxiliaries is obtained by multiplying the maximum power of the fans for the actual fraction of power:

$$P = \gamma P_{\max} \tag{A.4}$$

Data employed for the simulation are summarised in Table A.3:

Table A.3: Parameters for the cooling tower

Parameter	Value
Design inlet fluid temperature	38 °C
Design outlet fluid temperature	32°C
Design fluid flow rate	7000 kg/h
Design dry bulb ambient air temperature	35 °C
Design wet bulb ambient air temperature	27.8 °C
Design air flow rate	15 kg/s
Rated fan power	1.8 kW
Rated heat power	35 kW

Fan coil

Fan coil has been modelled with the method of bypass-fraction, consisting in the split of the air stream in two flows, one passing in the coil and exiting in saturated conditions, and the other bypassing the coil. Bypass fraction has been defined to 0.15.

Efficiency of the coil can be expressed as a function of bypass factor as:

$$BF = \frac{T_{entering\_coil} - T_{leaving\_coil}}{T_{entering\_coil} - T_{dewpoint}} \tag{A.5}$$

With T being dry bulb temperatures.

Pumps

Pumps have been modelled by means of Type110 of TRNSYS as variable speed pumps, that can provide any outlet mass flow rate between zero and a rated value. The mass flow rate provided by the pump varies

linearly with control signal. Efficiency of the pump can be modelled by using a polynomial expression, but in the present case only the first order coefficient has been employed. A summary of the pumps, the nominal flow rates and efficiency is given in Table A.4:

Table A.4: Features of the pumps for the modelled system

Pump	Nominal flow rate	Power consumption at nominal
Solar loop	1.25 kg/s	600 W
Hot water chiller	1.0 kg/s	150 W
Heat rejection chiller	1.38 kg/s	600 W
Low temperature chiller	0.42 kg/s	100 W

System management logic

For a solar cooling system, management is a key issue, strongly affecting its operation. In the present simulations, the following controls have been applied:

1. All the components of the system are turned on between 8.00 and 17.00.
2. The pump of the solar loop is turned on only when the temperature on the surface of solar collectors is higher than the temperature in the lower node of the tank.
3. The speed of the pump in the solar loop is varied continuously in order to maintain a constant temperature difference between the collectors and the tank (5°C). More specifically, the mass flow rate is varied linearly with the temperature difference between the tank and the solar collectors, according to an equation of this kind:

$$\dot{m} = a\Delta T + b \qquad \text{(A.6)}$$

   Where a and b are coefficient determined empirically through a first set of simulations, according to the approach described in [52]
4. The pump of the driving circuit of the adsorption chiller is turned on when the temperature inside the tank exceeds 60°C, which is the minimum driving temperature for the adsorption chiller.
5. The on/off and speed of the pump of the chilled water circuit are regulated in order to maintain the set-point temperature inside the office (26°C for cooling and 20°C for heating).

It is worth noticing that the maximum flow rate for the pump in the solar loop has been changed according to the total area of the field, with the aim of maintaining the maximum temperature level inside the tank almost constant (around 95°C) for all the considered simulations.

REFERENCES

[1] Sustainable Innovation Forum, report on Climate Commitments of Subnational Actors and Business, 2015, http://www.cop21paris.org/knowledge-centre/reports/

[2] Ren21, Renewables 2015 Global Status Report,2015, http://www.ren21.net/

[3] IPCC, Climate change synthesis report, IPCC Fourth Assessment Report (2007)

[4] N. Kalkan, E.A. Young, A. Celiktas, Solar thermal air conditioning technology reducing the footprint of solar thermal air conditioning, Renewable and Sustainable Energy Reviews 16 (2012), pp. 6352–6383.

[5] A. Kalogirou Soteris , Solar space heating and cooling. In: Kalogirou Soteris A, editor., Solar energy engineering. Boston: Academic Press; 2014. p. 323–95 [chapter 6].

[6] A. Allouhi , T. Kousksou, A. Jamil, P. Bruel, Y. Mourad, Y. Zeraouli, Solar driven cooling systems: An updated review, Renewable and Sustainable Energy Reviews 44(2015)159–181

[7] Advances in Solar Heating and Cooling, Edited by R.Z. Wang and T.S. Ge, Woodhead Publishing Series in Energy: Number 102, doi:10.1016/B978-0-08-100301-5.01001-8
[8]Solar Cooling Handbook – A Guide to Solar Assisted Cooling and Dehumidification Processes (3rd, completely revised edition), Ed. Hans-Martin Henning, Mario Motta, Daniel Mugnier, AMBRA 2013, ISBN 978-3990434383
[9] R.Z. Wang, T.S. Ge, C.J. Chen, Q. Ma, Z.Q. Xiong, Solar sorption cooling systems for residential applications: options and guidelines, International Journal of Refrigeration 32 (2009), pp. 638–660.
[10] B. Choudhury, P.K. Chatterjee, J.P. Sarkar, Review paper on solar-powered air-conditioning through adsorption route, Renewable and Sustainable Energy Reviews 14 (2010), pp. 2189–2195.
[11] K.F. Fong, T.T. Chow, C.K. Lee, Z. Lin, L.S. Chan, Advancement of solar desiccant cooling system for building use in subtropical Hong Kong, Energy and Buildings 42 (12) (2010), pp. 2386–2399.
[12] P. Finocchiaro, M. Beccali, B. Nocke, Advanced solar assisted desiccant and evaporative cooling system equipped with wet heat exchangers, Solar Energy 86 (2012), pp. 608–618.
[13] Q. Cheng, ,X. Zhang Review of solar regeneration methods for liquid desiccant air-conditioning system, Energy and Buildings 67)(2013), pp. 426–433
[14] W. Sparber, A. Napolitano, P. Melograno, Overview in worldwide installed solar cooling systems. In: 2nd International conference solar air conditioning, Tarragona – Spain; October, 2007, http://archive.iea-shc.org/publications/downloads/task38-Overview.pdf
[15] U. Jakob, Solar cooling technologies, in: G. Stryi-Hipp, editor, Renewable Heating and Cooling-Technologies and Applications, ISBN: 978-1-78242-213-6, Woodhead Publishing (UK) [Chapter 6]
[16] X.H. Li, X.H. Hou, X. Zhang, Z.X. Yuan, A review on development of adsorption cooling—Novel beds and advanced cycles, Energy Conversion and Management 94 (2015) 221–232
[17] M.S. Fernandes, G.J.V.N. Brites, J.J. Costa, A.R. Gaspar, V.A.F. Costa, Review and future trends of solar adsorption refrigeration systems, Renewable and Sustainable Energy Reviews 39 (2014), pp. 102–123
[187] F. Meunier, Adsorption heat powered heat pumps, Applied Thermal Engineering 61, Issue 2, (2013) pp.830–836
[19] A. N. Shmroukh, A.H. H. Ali, S.Ookawara, Adsorption working pairs for adsorption cooling chillers: A review based on adsorption capacity and environmental impact, Renewable and Sustainable Energy Reviews 50 (2015) pp. 445–456
[20]Sortech, www.sortech.de
[21] Invensor, www.invensor.de
[22] U. Eicker, D. Pietruschka, M. Haag, A. Schmitt, Systematic design and analysis of solar thermal cooling systems in different climates, Renewable Energy 80 (2015) 827-836
[23] U. Eicker, D. Pietruschka, M. Haag, A. Schmitt , Comparison of photovoltaic and solar thermal cooling systems for office buildings in different climates, Solar Energy 118 (2015) 243–255
[24] N. Hartmann, C. Glueck, F.P. Schmidt, Solar cooling for small office buildings: Comparison of solar thermal and photovoltaic options for two different European climates, Renewable Energy 36 (2011), Pages 1329–1338
[25] G. Mohan, U. Kumara, M.K. Pokhrel, , A. Martin, Applied Energy (2015), doi:10.1016/j.apenergy.2015.10.116
[26] S. Vasta, V. Palomba, A. Frazzica, F. Costa, A. Freni, Dynamic simulation and performance analysis of solar cooling systems in Italy, Energy Procedia 81 (2015) 1171 – 1183
[27] S. Vasta, V. Palomba, A. Frazzica, **.** Di Bella, A. Freni, Techno-Economic Analysis of Solar Cooling Systems for Residential Buildings in Italy, J. Sol. Energy Eng 138 (2016)
[28] F. Reda, M. Viot K. Sipilä, M. Helm, Energy assessment of solar cooling thermally driven system configurations for an office building in a Nordic country, Applied Energy 166 (2016) 27–43
[29] Ali M. Baniyounes, M.G. Rasul, M.M.K. Khan, Assessment of solar assisted air conditioning in Central Queensland's subtropical climate, Australia, Renewable Energy 50 (2013) 334-341

[30] A. Al-Alili, M.D. Islam, I. Kubo b, Y. Hwang, R. Radermacher, Modeling of a solar powered absorption cycle for Abu Dhabi, Applied Energy 93 (2012) 160–167
[31] J.P. Praene, O. Marc, F. Lucas, F. Miranville, Simulation and experimental investigation of solar absorption cooling system in Reunion Island, Applied Energy 88 (2011) 831–839
[32] J. Muye, D. S. Ayou, R. Saravanan, A. Coronas, Performance study of a solar absorption power-cooling system, Applied Thermal Engineering 97 (2016) 59–67
[33] A. Buonomano, F. Calise, M. Dentice d'Accadia, G.Ferruzzi, S. Frascogna, A. Palombo, R.russo, M. Scarpellino, Experimental analysis and dynamic simulation of a novel high-temperature solar cooling system, Energy Conversion and Management 109 (2016) 19–39
[34] A. Aliane, ,S. Abboudi, , C. Seladji, B. Guendouz, An illustrated review on solar absorption cooling experimental studies, Renewable and Sustainable Energy Reviews 65, 2016, Pages 443–458
[35] X.Q. Zhai, R.Z. Wang, J.Y. Wu, Y.J. Dai, Q. Ma, Design and performance of a solar-powered air-conditioning system in a green building, Applied Energy 85 (2008) 297–311
[36] X.Q. Zhai, R.Z. Wang, Experimental investigation and performance analysis on a solar adsorption cooling system with/without heat storage, Applied Energy 87 (2010) 824–835
[37] TRNSYS 17: a transient system simulation program, Solar Energy Laboratory, University of Wisconsin, Madison, USA.
[38] Tabula Web Tool, http://webtool.building-typology.eu/#pdfes
[39] P. V. Quiles, F. J. Aguilar, S. Aledo, Analysis of the Overheating and Stagnation Problems of Solar Thermal Installations, Energy Procedia 48 (2014) 172-180
[40] C. Stanciu, D. Stanciu, Optimum tilt angle for flat plate collectors all over the World – A declination dependence formula and comparisons of three solar radiation models, Energy Conversion and Management 81 (2014) 133–143
[41] S. Vasta, V. Palomba, D. La Rosa, G. Restuccia, A. Freni, Solar adsorption cooling system: development of a plant for air conditioning of a small office, Proc. of ASME-ATI-UIT 2015 Conference on Thermal Energy Systems: Production, Storage, Utilization and the Environment, Napoli, Italy, 17-20 May, 2015
[42] P. Taylor, O. Lavagne D'Ortique, N. Trudeau, M. Francoueur, Energy Efificency Indicators for Public Electricity Production from Frossil Fuels, IEA Information Paper, https://www.iea.org/publications/freepublications/publication/En_Efficiency_Indicators.pdf
[43] IEA Statistics, CO2 Emissions from Fuel Combustion (2015), ISBN 978-92-64-24595-2
[44] L. Zhao, W. Zeng, Z. Yuan, Reduction of potential greenhouse gas emissions of room air-conditioner refrigerants: a life cycle carbon footprint analysis, Journal of Cleaner Production 100,(2015), pp. 262–268
[45] I.P. Koronaki, D. Cowan, G. Maidment, K. Beerman, M. Schreurs, K. Kaar, I. Chaer, G. Gontarz, R.I. Christodoulaki, X. Cazauran, Refrigerant emissions and leakage prevention across Europe – Results from the RealSkills Europe project, Energy 45 (2012), pp. 71–80
[46]J.A. Duffie, W.A. Beckman, Solar Engineering of Thermal Processes, 2013, Wiley And Sons, ISBN 978-0-470-87366-3
[47] Z.S. Lu, R.Z. Wang, Z.Z. Xia, Q.B. Wu, Y.M. Sun, Z.Y. Chen,An analysis of the performance of a novel solar silica gel-water adsorption air conditioning, Applied Thermal Engineering 31 (2011) 3636-3642
[48] Wang DC, Xia ZZ, Wu JY, Wang RZ, Zhai H, Dou WD. Study of a novel silica gel–water adsorption chiller. Part I. Design and performance prediction. Int J Refrig. 2005;28:1073-83.
[49] Wang DC, Wu JY, Xia ZZ, Zhai H, Wang RZ, Dou WD. Study of a novel silica gel–water adsorption chiller. Part II. Experimental study. Int J Refrig. 2005;28:1084-91.
[50] B. Costelloe, D.P. Finn, Heat transfer correlations for low approach evaporative cooling systems in buildings, Applied Thermal Engineering 29 (2009) 105–115
[51] ASHRAE, ASHRAE Handbook: Systems and Equipment. ASHRAE, Atlanta, GA, 2000.

803 [52] L.M. Ayompe, A. Duffy, S.J. McCormack, M. Conlon, Validated TRNSYS model for forced circulation
804 solar water heating systems with flat plate and heat pipe evacuated tube collectors, Applied Thermal
805 Engineering 31 (2011) 1536-1542
806